

Maximum dc Josephson Current in Pb-PbO_x-Pb Junctions

K. Schwidtal and R. D. Finnegan

Institute for Exploratory Research, U. S. Army Electronics Command, Fort Monmouth, New Jersey 07703

(Received 26 January 1970)

We have measured the magnetic field dependence of the maximum dc Josephson current for square Pb-PbO_x-Pb Josephson junctions, with the ratio of junction width w to Josephson penetration depth λ_J as a parameter that was systematically varied. For wide Josephson junctions, the maximum dc Josephson current in zero external magnetic field I_0 is limited by the current-induced self-field, while for very narrow Josephson junctions, I_0 is limited by thermal noise. However, we have shown that for square Pb-Pb Josephson junctions with $1.00 > w/\lambda_J > 0.22$, the self-field as well as thermal noise is negligible. For these junctions, our experimental results are in consistent agreement with the theoretical prediction of Fulton and McCumber, who have shown that strong-coupling effects will reduce I_0 to 78.8% of the weak-coupling prediction for Pb-Pb junctions. We present evidence for the uniformity of our PbO_x tunneling barrier layers, and a model for the formation of our PbO_x layers.

I. INTRODUCTION

For a uniform narrow Josephson junction, i.e., a junction whose dimensions are small with respect to the Josephson penetration depth, the magnetic field dependence of the maximum tunneling supercurrent I_{\max} will be given by the simple expression¹

$$I_{\max} = I_0 \left| \frac{\sin(\pi\Phi/\Phi_0)}{\pi\Phi/\Phi_0} \right|. \quad (1)$$

Here Φ is the magnetic flux in the junction, Φ_0 is the quantum unit of magnetic flux, and I_0 is the maximum tunneling supercurrent in zero magnetic field. For a junction fabricated from a single superconducting material, that is a BCS or weak-coupling superconductor in which the gap parameter Δ is a real constant, I_0 is directly related to the normal tunneling resistance R_{NT} of the junction, the energy gap $\Delta(T)$, and the temperature²

$$I_{0w}(T) = [\pi\Delta(T)/2eR_{NT}] \tanh[\Delta(T)/2kT], \quad (2)$$

where the subscript w indicates the weak-coupling limit. Lead, however, is a strong-coupling superconductor, and Eq. (2) is not necessarily applicable to Pb-PbO_x-Pb junctions.

A general expression for $I_0(T)$, that is sufficiently general to apply to superconductors with strong electron-phonon coupling, was first derived by Ambegaokar and Baratoff.² For an identical superconductor junction it can be put in the form³

$$I_{0s}(T) = (\pi\Delta_0/2eR_{NT}) [\tanh(\Delta_0/2kT)] / [1 - \Delta'_1(\Delta_0)] - \frac{1}{eR_{NT}} \int_{\Delta_0}^{\infty} dw \tanh(w/2kT) \operatorname{Im} \left(\frac{\Delta^2(w)}{\omega^2 - \Delta^2(w)} \right). \quad (3)$$

Here the energy-gap parameter $\Delta(\omega)$ is a com-

plex function of the phonon energy E (or phonon frequency $\omega = E/\hbar$),

$$\Delta(\omega) = \Delta_1(\omega) + i\Delta_2(\omega), \quad \Delta'_1(\omega) = d\Delta_1(\omega)/d\omega,$$

Δ_0 is that value of ω for which $\omega = \Delta_1(\omega)$, and the subscript s indicates the strong-coupling limit. Recently, Fulton and McCumber³ have numerically evaluated Eq. (3) for Pb-Pb and for Sn-Sn junctions at $T=0$. Using published experimental data for $\Delta(\omega)$, and defining Δ_0 as the midpoint of the rise in tunneling current, they find that strong-coupling effects reduce I_0 to 78.8% of the weak-coupling prediction for lead:

$$I_{0s} = 0.788 I_{0w} \quad (4)$$

for Pb-Pb junctions. This relation is strictly valid only at $T=0$. But the deviation of the temperature dependence of the gap parameter for lead from the BCS expression is less than 2%,^{4,5} and within this limitation Eq. (4) may be assumed to be valid for all temperatures below the superconducting transition temperature of lead.

Most of the experimental data for I_0 that have been reported previously are far below the theoretically predicted value⁶⁻⁸; a value of approximately $0.8 I_{0w}$ has been reported only once.⁹ This may be explained by the influence of thermal noise. Even if all external effects that may reduce I_{\max} are excluded, a finite tunneling supercurrent can be observed only if the coupling energy associated with that current is larger than kT .¹⁰ In zero magnetic field, the coupling energy E_J of the junction that is associated with the tunneling supercurrent I_J is^{1,10,11}

$$E_J = -(\hbar/2e) I_0 \cos\varphi_0, \quad (5)$$

$$I_J = I_0 \sin\varphi_0, \quad (6)$$

where φ_0 is the difference of the quantum phases

of the gap functions on the two sides of the barrier. As $E_J \rightarrow 0$ when $I_J \rightarrow I_0$, the experimentally measured I_{\max} in zero magnetic field, I_{0m} , is not equal to, but less than I_0 , and is given by the condition that

$$I_J \rightarrow I_{0m} \text{ when } |E_J| \rightarrow |E_{\min}| > kT. \quad (7)$$

Eventually, when I_0 becomes less than $2ekT/\hbar$, no phase coherence can be established at all.

It is the purpose of the present study to experimentally determine the true value of I_0 for Pb-Pb Josephson junctions. We have measured the magnetic field dependence of I_{\max} for narrow square Pb-PbO_x-Pb Josephson junctions, with the ratio of junction width w to Josephson penetration depth λ_J as a parameter that was systematically varied. We shall show that between junctions that are too wide (I_0 reduced by self-field) and junctions that are too narrow (I_0 reduced by thermal noise) there is a range of junctions in the I_0 versus w/λ_J representation for which the self-field as well as the thermal noise can be neglected. From these junctions, the true value of I_0 can be determined. As the quality of the junctions and the noise seen by the junctions depend on the junction preparation and measurement techniques, respectively, these techniques will be described in some detail.

II. EFFECTS INFLUENCING MAXIMUM dc JOSEPHSON CURRENT

There are several effects that may modify the maximum tunneling supercurrents and that have to be avoided in order to measure the true I_0 :

(a) Tiny superconducting shorts will increase I_{\max} by the current necessary to drive the shorts normal. These shorts can be identified by a constant current superimposed on the magnetic field dependence pattern for narrow junctions.

(b) Stray magnetic and rf fields will reduce I_{0m} , and so will trapped flux. The junction therefore has to be carefully shielded, during operation as well as during the transition from the normal to the superconducting state. Also, the tunneling barrier layer must be uniform in order to prevent flux trapping in the junction whenever the current is reduced below I_{\max} .

(c) I_{0m} will also be reduced by tunneling transitions accompanied by spin reversal during the transition, caused, for example, by paramagnetic impurities in the tunneling barrier layer.¹²

(d) Assuming that all the above effects are eliminated, the junction still operates in the presence of the junction current, which may reduce I_{0m} by a current-induced magnetic self-field,¹³ or by thermal noise. These effects cannot be eliminated for a given junction; they can only be made negligible by a proper choice of the junction. We

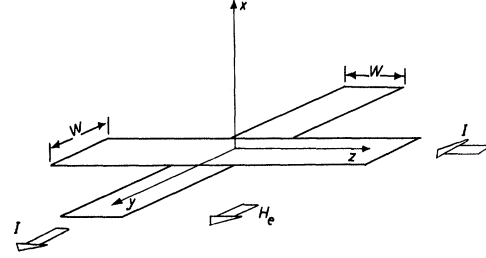


FIG. 1. Schematic drawing of a cross-type square Josephson junction. The arrows indicate the direction of the current in the film strips, and the direction of the externally applied magnetic field H_e .

will discuss these effects for the junction geometry shown in Fig. 1.

A. Magnetic Self-Field

For the geometry shown in Fig. 1, the ratio of junction width w to the Josephson penetration depth λ_J is

$$w/\lambda_J = (8\pi edI_{0s}/\hbar c^2)^{\frac{1}{2}} \quad (8)$$

and the magnetic flux Φ in the junction due to an externally applied magnetic field H_e is

$$\Phi_{e,y} = H_e w d. \quad (9)$$

Here $d = 2\lambda + t$, λ is the superconducting penetration depth of lead, and t is the barrier layer thickness.

Superimposed on the magnetic flux due to an externally applied magnetic field will be the magnetic flux due to the current-induced self-field. If we restrict our discussion to narrow junctions, the tunneling supercurrent density j_x can be assumed to be constant throughout the junction area. In this case, the current-induced magnetic self-field is

$$\begin{aligned} H_{\text{self},y}(z) &= -(4\pi/c)(I_x/w) \\ &= (4\pi/c)(I_{\max}/w)(z/w + \frac{1}{2}), \end{aligned} \quad (10a)$$

$$\begin{aligned} H_{\text{self},z}(y) &= -(4\pi/c)(I_y/w) \\ &= -(4\pi/c)(I_{\max}/w)(y/w + \frac{1}{2}). \end{aligned} \quad (10b)$$

By integrating over the cross section of the junction the magnetic flux due to the self-field is obtained:

$$\Phi_{\text{self},y} = (2\pi/c) d I_{\max}, \quad (11a)$$

$$\Phi_{\text{self},z} = (2\pi/c) d I_{\max}. \quad (11b)$$

By including the current-induced self-field, Eq.

(1) will therefore be modified to^{9,14}

$$I_{\max} = I_0 \left| \frac{\sin(\pi \Phi_{\text{self},z}/\Phi_0)}{\pi \Phi_{\text{self},z}/\Phi_0} \right|$$

$$\times \left| \frac{\sin[\pi(\Phi_{e,y} + \Phi_{self,y})/\Phi_0]}{\pi(\Phi_{e,y} + \Phi_{self,y})/\Phi_0} \right| \quad (12)$$

for narrow junctions. The maximum of the I_{max} versus H_e curve will no longer be at $H_e = 0$, but at a negative H_e that is given by the condition $-\Phi_{e,y} = \Phi_{self,y}$. The maximum tunneling super-current in zero externally applied magnetic field will then be^{9,14}

$$I_{0m} = I_0 \left(\frac{\sin(2\pi e d I_{0m} / \hbar c^2)}{2\pi e d I_{0m} / \hbar c^2} \right)^2. \quad (13)$$

From this equation, and using Eq. (8), one can obtain the relation

$$1 \geq \frac{I_{0m}}{I_0} \geq \left[\frac{\sin(w/2\lambda_J)}{(w/2\lambda_J)^2} \right]^2, \quad (14)$$

from which the upper limit of the reduction of I_{0m} due to the self-field can be estimated, as a function of w/λ_J . For $w/\lambda_J = 1$, I_{0m} will be $0.98 I_0 < I_{0m} < I_0$, and the deviation of I_{0m} from I_0 will decrease with decreasing w/λ_J . For $w/\lambda_J = 0.50$, I_{0m} will be $0.999 I_0 < I_{0m} < I_0$.

Thus for junctions with $w/\lambda_J \leq 1$, Eq. (1) will represent the magnetic field dependence with an error of less than 2% if one considers the magnetic flux due to an externally applied magnetic field only.

B. Thermal Noise

When the coupling energy E_J of the junction is not $|E_J| > kT$, then thermal fluctuations can disrupt the phase coherence across the barrier layer,¹⁰ and the dc Josephson current will acquire a noise voltage with a nonzero average value. This noise voltage has recently been analyzed theoretically^{15, 16} and experimentally.¹⁷ For low temperatures, however, where the junction resistance R_J for voltages $V < \Delta$ is $R_J \gg R_{NT}$, these theories do not apply. For this case quantitative data for I_{0m} with respect to I_0 can be obtained by defining an effective noise temperature T_n so that

$$I_J \rightarrow I_{0m}, \text{ when } |E_J| \rightarrow |E_{min}| = kT_n. \quad (15)$$

$$\text{Then } |\cos \varphi_{0, min}| = 2ekT_n / \hbar I_0 \quad (16)$$

$$\text{and } I_{0m} = [I_0^2 - (2ekT_n / \hbar)]^{1/2}. \quad (17)$$

The noise temperature is not necessarily the junction temperature since thermal noise is transmitted to the junction down the leads to the cryostat from room-temperature circuitry. Also, T_n is not strictly a temperature, but a parameter that is defined by Eq. (15), and that also depends on the junction resistance, inductance, and capacitance. Nevertheless, this parameter T_n will serve the purpose to obtain an estimate of the reduction of I_{0m} due to thermal noise. If we assume T_n to be

300°K, then I_{0m} will be $I_{0m} \geq 0.98 I_0$ for $w/\lambda_J \geq 0.16$, and $I_{0m} \geq 0.999 I_0$ for $w/\lambda_J \geq 0.33$. For the unlikely high noise temperature of $T_n = 1000^\circ\text{K}$, the corresponding data would be $I_{0m} \geq 0.98 I_0$ for $w/\lambda_J \geq 0.28$, and $I_{0m} \geq 0.999 I_0$ for $w/\lambda_J \geq 0.60$. An upper limit for T_n for the actual experimental situation can be obtained from a plot of experimentally obtained I_{0m} -versus- w/λ_J data by finding the best fit of Eq. (17) to the experimental data.

C. True Maximum dc Josephson Current

From the above considerations it follows that even for the unlikely high noise temperature of 1000°K, there still is the range $1.0 > (w/\lambda_J) > 0.3$ in the I_0 -versus- w/λ_J representation, in which the measured maximum tunneling super-current I_{0m} will agree with the theoretical value I_0 to better than 2%. The range $1.0 > (w/\lambda_J) > 0.3$ approximately corresponds to the junction resistance range $0.6 \Omega < R_{NT} < 6.4 \Omega$. This resistance range is large enough to unambiguously measure the "true" I_0 .

III. EXPERIMENTAL TECHNIQUES

A. Junction Preparation

Our Josephson junctions consisted of a lead-oxide barrier layer sandwiched between crossed perpendicular strips of lead films that were about 2000 Å thick and 0.30 mm wide, thus forming a square junction area (Fig. 1). Three parallel junctions were usually prepared on a 1-in. square substrate of Corning 7059 glass (Fig. 2) by first condensing three parallel bottom lead strips in a conventional diffusion-pumped vacuum system, oxidizing these strips to form the tunneling-barrier layers, and completing the junction by con-

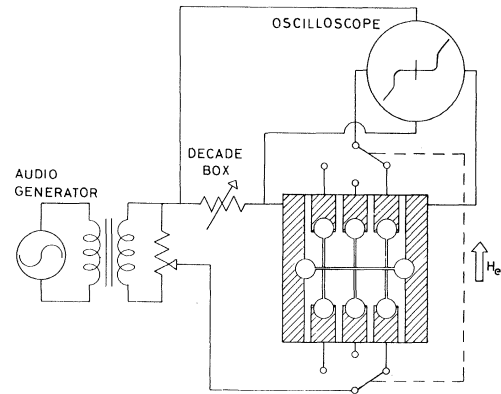


FIG. 2. Circuit for measuring the I-V characteristics, and substrate (to scale) with three Josephson junctions.

densing one common top lead strip perpendicular to the bottom strips. The vacuum during evaporation was in the low 10^{-6} -Torr range, and the evaporation rate was about $75 \text{ \AA}/\text{sec}$. Solderable contacts were provided by condensing silver-manganese dots¹⁸ onto the substrate prior to preparing the junctions. A mask-substrate changer was employed to avoid substrate exposure to the atmosphere between preparation steps.

The preparation of satisfactory lead-oxide tunneling-barrier layers is made difficult by the inherent properties of thin lead-oxide films. The reaction of oxygen with evaporated films of lead results in an orthorhombic lead-monoxide layer,¹⁹ which is an oxygen-deficiency (*n*-type) semiconductor.^{19, 20} In contact with oxygen pressures larger than about 10^{-2} Torr, the surface of the lead-oxide layer will become *p* type,^{19, 20} and a *n-p* contact barrier is formed.²⁰ From this model one would expect that it will be difficult to modify the width of the effective barrier layer and that one is limited in the range of junction resistivities when the oxidation of the bottom lead strips is done by thermal oxidation. We, therefore, used the following procedure for oxidizing the bottom lead strips, which gave us most satisfactory results. The bottom lead strips were first exposed to 20 mTorr O₂ for about 10 min; the substrate was left at room temperature. During this exposure, an about 30-Å-thick saturation layer of *n*-type lead monoxide should be formed.¹⁹ Subsequently, a glow discharge between the substrate holder and a disk-shaped aluminum cathode was maintained in the same O₂ ambient for 20 to 30 sec. The glow current density was about $10^{-5} \text{ A}/\text{cm}^2$, and the duration of the glow determined the junction resistance. This technique is usually referred to as "plasma anodization."²¹ However, even if we assume an ion yield of 2, i.e., each electron reaching the Pb/PbO_x film will give rise to one PbO molecule, the increase in junction resistance with glow time cannot be explained by an increase in oxide layer thickness alone. We, therefore, assume that the glow discharge serves mainly to dope the existing oxide layer with oxygen. This doping will increase the spacing between the Fermi level and the conduction band, and will therefore increase the barrier height.

It should be noted that this model is applicable only for the very conditions under which our oxidation was carried out. For different conditions, like higher oxygen pressure or higher temperature, the situation may be different, as the stoichiometry of thin lead-oxide films depends strongly on the ambient oxygen pressure and on temperature.²⁰ For example, Schroen²² has reported barrier layers, formed on lead films by a glow discharge oxidation technique, which could be

stored at room temperature for several months, whereas our junctions would deteriorate within a few days when stored at room temperature. Therefore, we had to cool our junctions down to liquid-helium temperature immediately after preparation. But this inconvenience was more than compensated by the advantages of our technique. We have been able to prepare junctions with resistance values ranging from $< 10^{-5} \Omega$ to $> 100 \Omega$, and with very low "excess currents."²³

B. Measurements

The substrate was mounted on a nylon sample holder at the end of a stainless-steel tube and in the center of a 4-in.-long solenoid that produced a magnetic field, parallel to the bottom lead strips. The solenoid was surrounded by a Mu-metal can, which reduced the ambient magnetic field to less than 10^{-2} Oe. The tunneling-current-versus-voltage characteristics were displayed on an X-Y oscilloscope; the circuitry is shown in Fig. 2. The major advantage of this technique over a dc technique is that current fluctuations can be seen directly on the scope. The frequency of the audio generator was chosen so that the junction and circuit stray inductance was equal to the capacitance. This frequency was typically between 800 and 1200 Hz. The maximum tunneling-supercurrent-versus-magnetic-field curves were obtained by increasing the magnetic field in steps of 5×10^{-2} Oe, each time reading the maximum tunneling supercurrent on the X-Y scope. The normal tunneling resistance R_{NT} was taken as the limiting large voltage resistance when the lead films were superconducting, and was usually measured at $V = 20 \text{ mV}$.

IV. EXPERIMENTAL RESULTS

A. I-V Characteristics and Magnetic Field Dependence

Figure 3 shows typical current-versus-voltage characteristics at two different temperatures for the same junction. [The magnetic field dependence of the same junction is shown in Fig. 4(b)]. Within the resolution of our circuitry, we have never been able to see in the I-V characteristics the step at $V = \Delta$ which has been associated with multi-particle tunneling.²³ Subharmonic structures were seen in the I-V characteristics for some junctions, and the maxima in the magnetic field dependence for these junctions would decrease at a slower rate than predicted by Eq. (1). We take this as a further evidence that the subharmonic structure is associated with non-uniform tunneling-barrier layers.^{23, 24} However, in the final analysis of the "true" I_0 , we will include only junctions for which the magnetic field dependence followed a

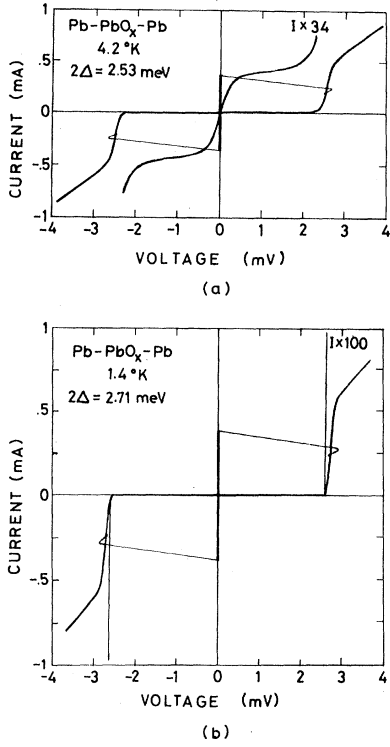


FIG. 3. Typical I-V characteristics of a Pb-PbO_x-Pb Josephson junction in zero externally applied magnetic field.

Fraunhofer diffraction pattern strictly. In the latter case, the tunneling barrier layer can be assumed to be uniform.

Figure 4 shows the magnetic field dependence of the maximum tunneling supercurrent I_{\max} for two different junctions. In Fig. 4 (a), $w/\lambda_J = 1.10$, and the maximum of the I_{\max} -versus- H_e curve has been shifted from $H_e = 0$ to a small negative value of H_e due to the current-induced self-field. In Fig. 4(b), the "pinching-off" of the I_{\max} -versus- H_e curve near the minima is caused by thermal noise.

From the periodicity of the I_{\max} -versus- H_e curve, $d = 2\lambda + t$ can be calculated. I_{\max} goes to zero whenever $\Phi = w d H_e$ is a multiple of Φ_0 . From the periodicity shown in Fig. 4, and $w = 0.30$ mm, it follows that

$$d = 1030 \pm 10 \text{ \AA}, \text{ at } 1.4^\circ \text{K}.$$

The theoretical value for the penetration depth of lead at $T = 0$ is $\lambda(\text{Pb}, T=0) = 480 \text{ \AA}$.²⁵ Using this value, we have to assume the thickness of the lead-oxide layer to be $t = 70 \pm 10 \text{ \AA}$. This value is larger than the $10 - 20 \text{ \AA}$ that is usually assumed for the thickness of the tunneling barrier layer in Josephson junctions. Considering the

peculiarities of lead-oxide films, however, this larger value seems reasonable.

Once d is known, the relation between w/λ_J and R_{NT} can be calculated, using Eqs. (8), (4), and (2):

$$w/\lambda_J = 0.810/[R_{NT}(\Omega)]^{\frac{1}{2}} \quad \text{at } 1.4^\circ \text{K},$$

$$w/\lambda_J = 0.779/[R_{NT}(\Omega)]^{\frac{1}{2}} \quad \text{at } 4.2^\circ \text{K},$$

for square Pb-PbO_x-Pb Josephson junctions, regardless of width w .

B. Effective Noise Temperature T_n

To determine the effective noise temperature T_n , we have measured I_{0m} for a series of junctions for which the junction resistance R_{NT} was systematically varied. The results are shown in Fig. 5, where I_{0m} is plotted versus R_{NT} in a logarithmic representation. The effective noise temperature T_n is obtained by fitting Eq. (17) to the experimental data. For our experimental conditions, T_n turns out to be in the range $450 - 600^\circ \text{K}$. Using

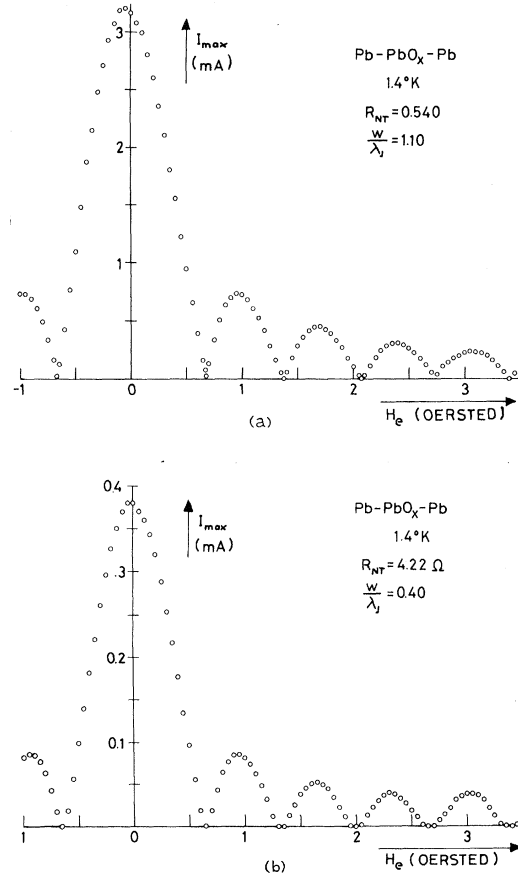


FIG. 4. The dependence of the maximum tunneling supercurrent I_{\max} on the externally applied magnetic field H_e .

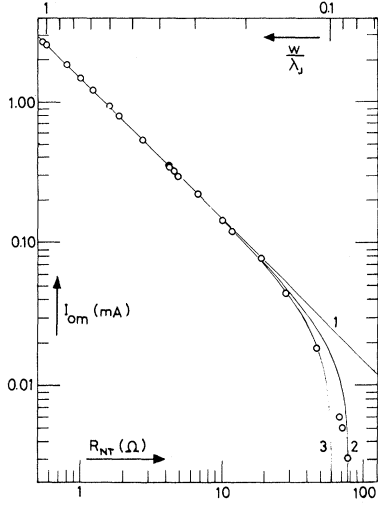


FIG. 5. The dependence of the maximum tunneling supercurrent in zero externally applied magnetic field I_{0m} on the normal tunneling resistance R_{NT} and w/λ_J at 4.2°K. The open circles are experimental results. Curve 1 represents I_{0s} , while curves 2 and 3 represent I_{0m} , Eq. (17), with a thermal noise temperature T_n of 450 and 600°K, respectively.

the upper limit $T_n = 600$ °K, the measured I_{0m} will then be $I_{0m} \geq 0.98 I_0$ for $w/\lambda_J \geq 0.22$, and will be $I_{0m} \geq 0.999 I_0$ for $w/\lambda_J \geq 0.46$ if the reduction of the maximum tunneling supercurrent caused by thermal noise only is considered.

C. True Maximum dc Josephson Current I_0

In the preceding sections, we have shown that for our experimental conditions, the measured maximum tunneling supercurrent in zero external magnetic field I_{0m} will agree with the theoretical value I_0 to within better than 2% in the range $1.0 > w/\lambda_J > 0.22$, and in the range $0.50 > w/\lambda_J > 0.46$ the agreement will even be better than 0.1%. We have also shown that our junctions can reasonably be assumed to be uniform. Therefore, we are now able to determine the "true" I_0 from our experimental data.

We have measured I_{0m} , and calculated I_{0m}/I_{0w} , for 16 junctions in the range $1.1 > w/\lambda_J > 0.2$ at 4.2°K; and for seven of them also at 1.4°K. The results are shown in Fig. 6. The maximum experimental error has been calculated by error-propagation theory from the maximum experimental errors in measuring I_{0m} , R_{NT} , $\Delta(T)$, and T . (For the sake of graphical clarity, we show in Fig. 6 the maximum experimental error for one data point only; it is representative for all of the I_{0m}/I_{0w} data points.) As an average, we obtain $I_{0m}/I_{0w} = 0.794 \pm 0.005$ at 4.2°K and

$I_{0m}/I_{0w} = 0.779 \pm 0.005$ at 1.4°K. We have also calculated the "true" I_0 corresponding to each I_{0m} , using Eq. (17) in the form

$$I_0 = [I_{0m}^2 + (2ekT_n/\hbar)^2]^{1/2}, \quad (18)$$

with $T_n = 600$ °K, to correct for the reduction of I_{0m} due to thermal noise for the range $w/\lambda_J < 0.46$; and using Eq. (14) in the form

$$I_0 = I_{0m} \left[\frac{1}{2}(1+a) + \frac{1}{2}(a-1) \right], \quad (19)$$

$$a = \left(\frac{(w/2\lambda_J)^2}{\sin(w/2\lambda_J)} \right)^2,$$

to correct for the reduction of I_{0m} due to the current-induced magnetic self-field for the range $w/\lambda_J > 0.50$. The results are also shown in Fig. 6. We obtain as an average

$$I_0 = (0.789 \pm 0.004) I_{0w} \quad \text{at } 4.2^\circ\text{K},$$

$$I_0 = (0.784 \pm 0.006) I_{0w} \quad \text{at } 1.4^\circ\text{K}.$$

As the difference of the energy gaps at $T = 0$ °K and $T = 1.4$ °K is negligible, the value at 1.4°K can be considered as representing the case $T = 0$. Within the limits of experimental error, this value is in excellent agreement with the strong-coupling prediction, $I_{0s} = 0.788 I_{0w}$. For the value at 4.2°K, we have to consider that the BCS temperature dependence of the energy gap has been

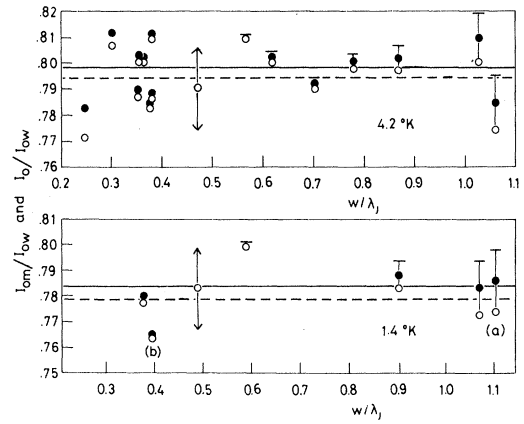


FIG. 6. I_{0m}/I_{0w} (open circles) and I_0/I_{0w} (full circles) versus w/λ_J at 4.2 and at 1.4°K. The w/λ_J axes are scaled so that for each junction the 1.4°K data point lies exactly below the 4.2°K data point. The dashed line represents $\langle I_{0m}/I_{0w} \rangle_{av}$, and the full line represents $\langle I_0/I_{0w} \rangle_{av}$. The arrowed bar indicates the maximum limit of experimental error, and is representative for all of the data points. The T bars indicate the error limits according to Eq. (19). (a) and (b) indicate those junctions for which the magnetic field dependence is shown in Figs. 4 (a) and 4 (b).

assumed, whereas for lead there are deviations from the BCS temperature dependence of maximum 2%.

V. CONCLUSIONS

We have measured the magnetic field dependence of the maximum tunneling supercurrent I_{\max} for narrow square Pb-PbO_x-Pb Josephson junctions, with the ratio of junction width w to the Josephson penetration depth λ_J as a parameter that was systematically varied. We show that for our experimental conditions, the measured maximum tun-

neling supercurrent in zero external magnetic field I_{0m} will agree with the theoretical value I_0 to within better than 2% in the range $1.0 > w/\lambda_J > 0.22$. From measurements of I_{0m} in this range we obtain that $I_0 = (0.784 \pm 0.006) I_{0w}$ at 1.4°K, where I_{0m} is the weak-coupling prediction for I_0 , $I_{0w} = \pi \Delta / 2eR_{NT}$ at 1.4°K. This result is in excellent agreement with the theoretical prediction of Fulton and McCumber, who have shown that strong-coupling effects will reduce I_0 to 78.8% of the weak-coupling prediction for Pb-Pb junctions.

-
- ¹B. D. Josephson, Rev. Mod. Phys. **36**, 216 (1964).
²V. Ambegaokar and A. Baratoff, Phys. Rev. Letters **10**, 486 (1963); **11**, 104 (E) (1963).
³T. A. Fulton and D. E. McCumber, Phys. Rev. **175**, 585 (1968).
⁴J. C. Swihart, D. J. Scalapino, and Y. Wada, Phys. Rev. Letters **14**, 106 (1965).
⁵R. F. Gasparovic, B. N. Taylor, and R. E. Eck, Solid State Commun. **4**, 59 (1966).
⁶J. M. Rowell, Phys. Rev. Letters **11**, 200 (1963).
⁷R. E. Eck, D. J. Scalapino, and B. N. Taylor, Phys. Rev. Letters **13**, 15 (1964).
⁸A. A. Galkin, B. U. Borodai, V. M. Svistunov, and V. N. Tarasenko, Zh. Eksperim. i Teor. Fiz. Pis'ma v Redaktsiya **8**, 521 (1968) [Soviet Phys. JETP Letters **8**, 318 (1968)].
⁹K. Schwidtal and R. D. Finnegan, J. Appl. Phys. **40**, 2123 (1969).
¹⁰P. W. Anderson, in *Lectures on the Many-Body Problem*, edited by E. R. Caianello (Academic, New York, 1964), Vol. 2, p. 113.
¹¹B. D. Josephson, Advan. Phys. **14**, 419 (1965).
¹²I. O. Kulik, Zh. Eksperim. i Teor. Fiz. **49**, 1211 (1965) [Soviet Phys. JETP **22**, 841 (1966)].
¹³R. A. Ferrell and R. E. Prange, Phys. Rev. Letter **10**, 479 (1963).
¹⁴T. Yamashita and Y. Onodera, J. Appl. Phys. **38**, 3523 (1967).
¹⁵V. Ambegaokar and B. I. Halperin, Phys. Rev. Letters **22**, 1364 (1969).
¹⁶Yu. M. Ivanchenko and L. A. Zil'berman, Zh. Eksperim. i Teor. Fiz. Pis'ma v Redaktsiya **8**, 189 (1968) [Soviet Phys. JETP Letters **8**, 113 (1968)].
¹⁷J. T. Anderson and A. M. Goldman, Phys. Rev. Letters **23**, 128 (1969).
¹⁸P. R. Gould and J. J. Finnegan, Rev. Sci. Instr. **33**, 767 (1962).
¹⁹J. R. Anderson and V. B. Tare, J. Phys. Chem. **68**, 1482 (1964).
²⁰L. Heijne, J. Phys. Chem. Solids **22**, 207 (1961); Philips Res. Repts. Suppl. No. 4 (1961).
²¹J. L. Miles and P. H. Smith, J. Electrochem. Soc. **110**, 1240 (1962).
²²W. Schroen, J. Appl. Phys. **39**, 2671 (1968).
²³J. M. Rowell and W. L. Feldmann, Phys. Rev. **172**, 393 (1968).
²⁴S. M. Marcus, Phys. Letters **19**, 623 (1966); **20**, 236 (1966).
²⁵J. Bardeen and J. R. Schrieffer, in *Progress in Low-Temperature Physics*, edited by C. J. Gorter (North-Holland, Amsterdam, 1961), Vol. 3, p. 170.